# NASA TECHNICAL MEMORANDUM



NASA TM 78191

# EVALUATION OF AAFE APPARATUS TO MEASURE RESIDUAL AND TRANSIENT CONVECTION IN ZERO-GRAVITY

By R. C. Ruff, B. R. Facemire, and W. K. Witherow
Space Sciences Laboratory

August 1978

NASA

*George C. Marshall Space Flight Center*
*Marshall Space Flight Center, Alabama*

TECHNICAL REPORT STANDARD TITLE PAGE

| 1. REPORT NO. | 2. GOVERNMENT ACCESSION NO. | 3. RECIPIENT'S CATALOG NO. |
|---|---|---|
| NASA TM-78191 | | |

| 4. TITLE AND SUBTITLE | 5. REPORT DATE |
|---|---|
| Evaluation of AAFE Apparatus to Measure Residual and Transient Convection in Zero-Gravity | August 1978 |
| | 6. PERFORMING ORGANIZATION CODE |
| 7. AUTHOR(S) R. C. Ruff, B. R. Facemire, and W. K. Witherow | 8. PERFORMING ORGANIZATION REPORT # |
| 9. PERFORMING ORGANIZATION NAME AND ADDRESS<br>George C. Marshall Space Flight Center<br>Marshall Space Flight Center, Alabama 35812 | 10. WORK UNIT NO. |
| | 11. CONTRACT OR GRANT NO. |
| | 13. TYPE OF REPORT & PERIOD COVERED |
| 12. SPONSORING AGENCY NAME AND ADDRESS<br>National Aeronautics and Space Administration<br>Washington, D.C. 20546 | Technical Memorandum |
| | 14. SPONSORING AGENCY CODE |

15. SUPPLEMENTARY NOTES

Prepared by Space Sciences Laboratory, Science and Engineering

16. ABSTRACT

This report presents the results of an evaluation of an apparatus built by the Jet Propulsion Laboratory under Advanced Applications Flight Experiment (AAFE) program funding. The results are expected to contribute to an improved design for a Fluid Experiments System (FES) planned for Spacelab 3. The detailed results are presented in four categories: (1) human factors, (2) electrical and mechanical, (3) optical performance, and (4) thermal performance.

| 17. KEY WORDS | 18. DISTRIBUTION STATEMENT |
|---|---|
| | NASA Headquarters and Centers Only |

R C Ruff

| 19. SECURITY CLASSIF. (of this report) | 20. SECURITY CLASSIF. (of this page) | 21. NO. OF PAGES | 22. PRICE |
|---|---|---|---|
| Unclassified | Unclassified | 36 | NTIS |

# ACKNOWLEDGMENTS

The authors wish to acknowledge the help of Dr. Paul Shlichta (JPL) and Dr. Roger Kroes (SSL, MSFC). Dr. Shlichta provided background and insight into operation of the AAFE system. Dr. Kroes provided the optical absorption measurements.

# TABLE OF CONTENTS

# LIST OF ILLUSTRATIONS

TECHNICAL MEMORANDUM 78191

# EVALUATION OF AAFE APPARATUS TO MEASURE RESIDUAL AND TRANSIENT CONVECTION IN ZERO-GRAVITY

## I. INTRODUCTION

A Fluids Experiments System (FES) is planned for Spacelab 3. This system will provide principal investigators with an optical system for photographing convective and diffusive flows in crystal growth experiments. This concept is an outgrowth of an Advanced Applications Flight Experiment (AAFE) developed jointly by Jet Propulsion Laboratory (JPL) and Dr. Paul Shlichta during the period of Dr. Shlichta's association with the University of Southern California.

This report documents a scientific evaluation of the engineering model built by JPL under AAFE funding. Many of the problems described were also found by JPL and would have been either corrected or at least documented if additional funds from the AAFE program had been available. This report is, therefore, an effort to document the performance capability of this engineering model and provide suggestions for improvements which should be incorporated in the FES for Spacelab 3.

Figure 1 is a photograph of the experimental apparatus associated with the AAFE experiment as delivered to Marshall Space Flight Center (MSFC) by JPL. Figure 2 is the associated electronic instrumentation. Figure 3 is a schematic of the system detailing the optical path followed in Figure 1.

The experiment concept is basically simple. A collimated white light is transmitted through the test cell. A processor wheel is then used to insert various optical elements in the beam before the image is photographed. These optical elements are monochromatic filters, a schlieren knife edge, and a Wollaston interference prism. These elements are expected to provide an investigator with the ability to separate effects from thermal and concentration gradients. Concentration gradients would be determined by measuring monochromatic absorption at selected wavelengths. Thermal gradients would be determined by deducting the effect of concentration gradients from the total index of refraction gradients measured with the interference and schlieren components. In addition to controls for the optical system, the electronics console contains temperature measurement and control equipment for the test cell.

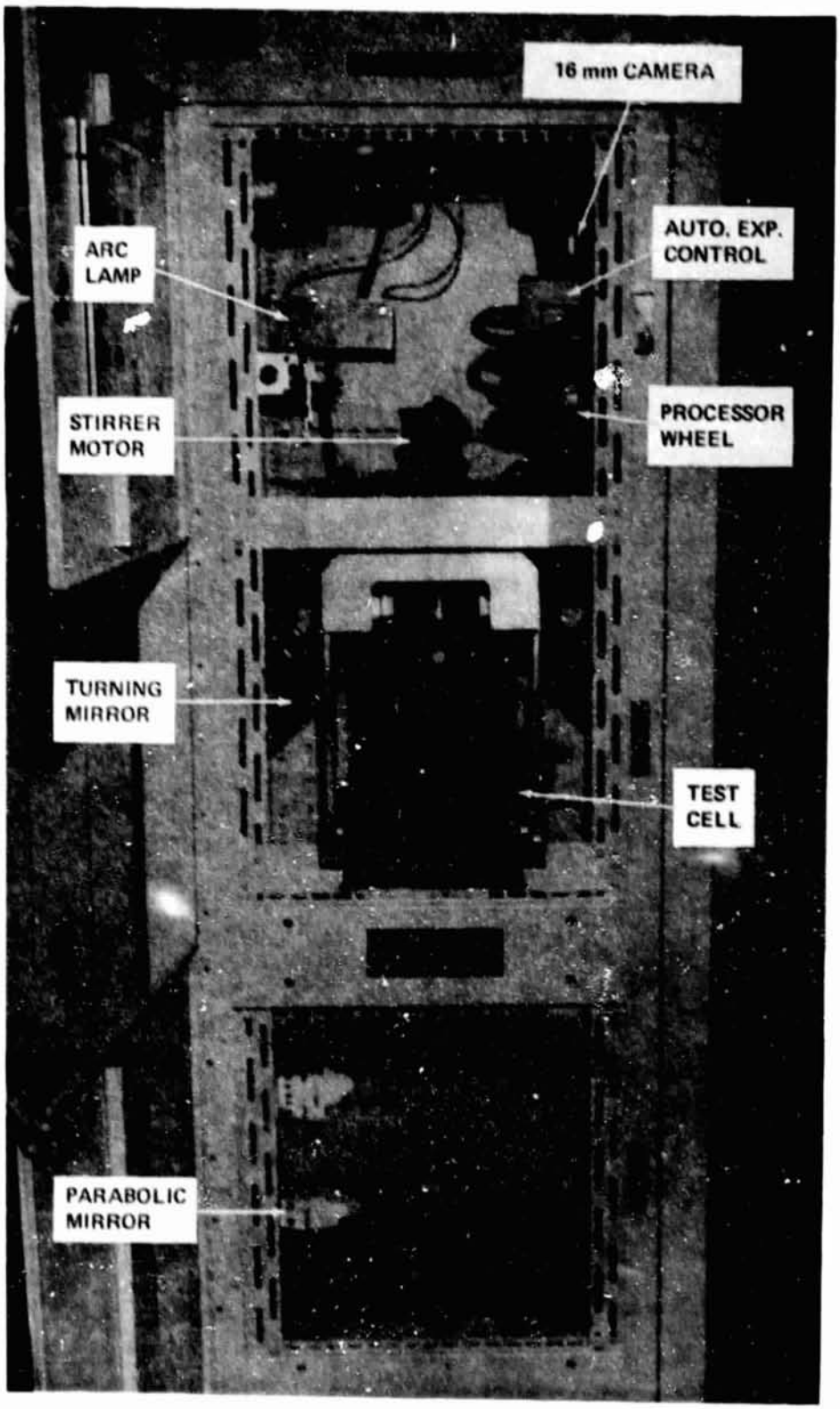


Figure 1. AAFE engineering model.

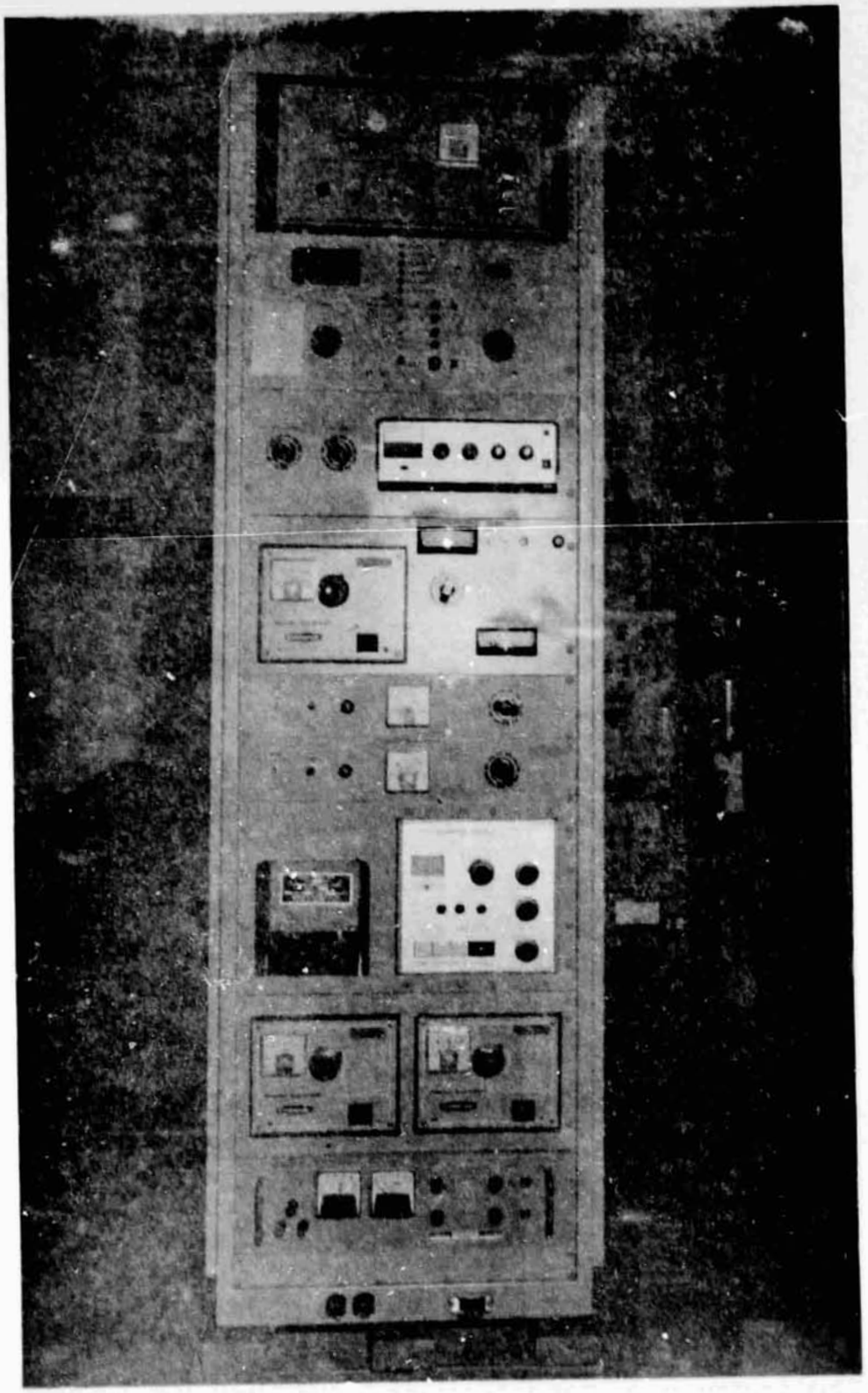

Figure 2. Electronic instrumentation associated with AA7E apparatus.

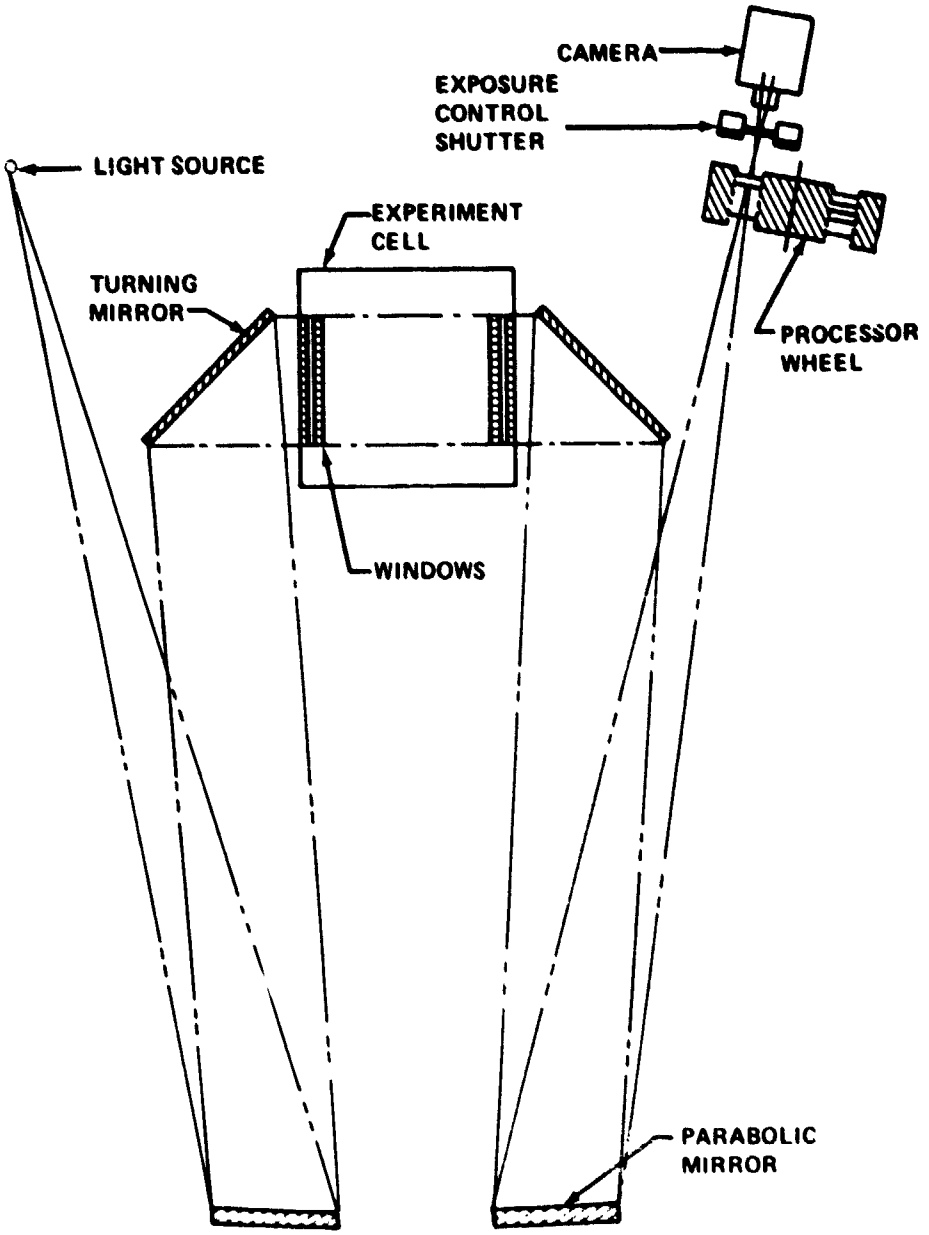


Figure 3. Optical schematic of AAFE apparatus.

# II. OBSERVATIONS AND HUMAN FACTORS

As a result of operating the AAFE engineering model, several observations were made which relate to operational procedures and human factors in general. These factors do not limit the capabilities of the instrument as a research tool but would severely hinder or limit results returned from an orbital facility if not considered.

## A. Realignment of Optics

Although the number of optical components is limited, as is seen in Figure 3, realignment is extremely complicated when approached for the first time with no guidance. While trying to determine the uniformity of illumination of the system, several components were moved which resulted in the generation of a large amount of coma aberration in the light beam. Several hours were required to learn how to adjust the system for minimum coma. Obviously, the time for realignment will be much shorter the next time it becomes necessary. The lesson learned, however, is that a Payload Specialist for Spacelab operation of such a system must be trained in alignment procedures. This should guarantee that a minimum of experiment time in orbit will be lost if alignment is necessary for whatever reason.

## B. Arc Lamp Operation

Two observations were made about arc lamp operation. The least significant has to do with the arc lamp igniter circuit. The Hanovia lamp supplied utilizes a spark gap discharge to ignite the lamp. The spark gap separation is critical and erodes with usage and conceivably could change with mechanical vibration during launch. With the possibility of a need to readjust this gap, it becomes imperative that the adjustment mechanism be made available at the front panel.

A second observation was that the Hanovia lamp has a preferred vertical orientation. According to a Hanovia engineer, the lamp becomes unstable as to arc position if operated upside down. It appears that convective currents in the arc are important at one-gravity; it is not known whether reduction of convective currents in space would benefit or hinder operation of this lamp.

## C. Processor Control Mechanism

The AAFE unit was designed to photograph six different phenomena in sequence by rotating the processor wheel in six increments. This objective was accomplished, and the sequence requires 12 s before repeating. However, for development testing and for versatility of experiment protocol in space, it should at least be possible to disable the processor and still activate the single-frame exposure mechanism to enable photography of a single parameter. At present, there is no ability to change the framing rate. Also, any movies taken will need to be sent to a commercial processing lab for separation into the six individual movies of independent parameters.

## D. Camera System

A procedure for focusing of the camera had to be developed. As will be shown in a later section, during a test to determine the maximum object resolution it was discovered that the camera must be set to a focus distance of 5 m. Using the boresight focusing mechanism supplied with the Photosonics 16 mm camera, it was impossible to find the optimum focus position when viewing only the crystal growth test cell. By replacing the test cell with a high-resolution test chart, one can learn to focus with reasonable accuracy. The limitation appears to be that the ground glass screen of the boresight has less resolution than desired. No suggestion on how to eliminate this problem can be made at this time.

The location of the camera made removal of the film magazine through the overhead panel of the relay rack very difficult. Also, the position of the boresight viewer necessitated use of a stepping stool for focus adjustment. Not only is this inconvenient, but it is impossible to do without jarring the entire system. The suggestion for improvement is to give the camera position a high priority during design tradeoff studies.

## E. Temperature Measurement and Control

This topic will be covered in detail in a later section; however, there were two features which led to extra labor in experiment setup and data reduction. First, all of the temperature measurements are in degrees Fahrenheit, which resulted in an immense number of conversions to the NASA-recommended SI units of degrees Celsius. The second factor was a temperature control system which utilized an arbitrary scale for the temperature set point.

It is recommended that for the FES all measurements and set points be direct reading. This not only eliminates a source of error, but it also minimizes confusion for all of the people who will interact with the unit from development testing through postflight analysis.

## F. Data Display on Film

The technique used in the AAFE unit to relate processor wheel position to film frame was to photograph a coded array of lights on each frame. However, this does not provide the degree of control of intensity needed for the multipurpose processor wheel. Under most conditions the lights were too dim to be visible on the film when developed. Recommendations for the FES are either to incorporate a light intensity control if data are photographed simultaneously with the test cell or to put data directly on the film, bypassing the lenses and shutter.

## G. Crystal Growth Techniques

Primarily, only one of the two test cells provided with the AAFE unit has been operated. This test cell was designed to utilize a sting for nucleating and growing a crystal at the center of the cell. This sting has not proved very reliable as a nucleation device. Also, when a crystal does emerge from the end of the sting, the thermal environment is such that the growing crystal engulfs the entire sting. Both of these problems were recognized by Dr. Shlichta, who is already looking for improvements for possible use in his Spacelab 3 experiment.

Other techniques not associated with the basic test cell which will need to be designed by principal investigators are such items as seed insertion and crystal removal mechanisms, bubble removal or control mechanisms, and temperature probes in the liquid.

The second test cell incorporates two thermoelectrically controlled isothermal plates for generating thermal gradients in the fluid. A series of interference photographs showing the effect of a horizontal gradient is shown in Figure 4. Only the left side of the cell was heated. The fluid in the test cell was a sucrose solution with a linear change in concentration from 1.5 wt. % at the bottom to pure water at the top. The solution was stable at the beginning of the test, and convective cells can be seen to start and grow at the heated wall.

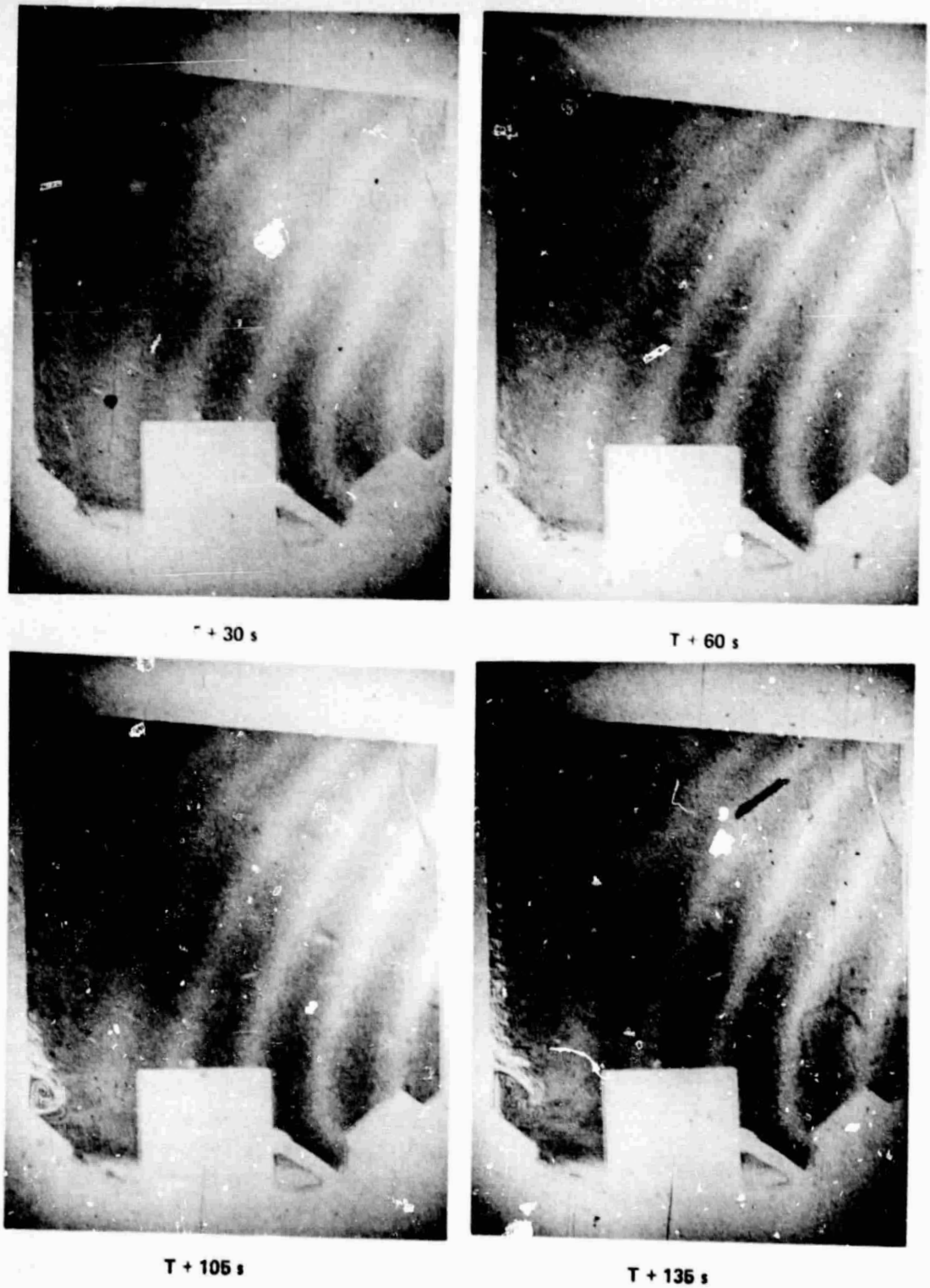


Figure 4. Series of interference photographs showing onset of convection.

It can be seen that this configuration of thermally controlled plates at the sides of a test cell is inappropriate for testing at one-gravity. Since there is no provision in the test cell holder for turning the cell on its side, no quantifiable measurements could be made to study index of refraction changes due to planar thermal gradients.

## III. MECHANICAL AND ELECTRICAL PROBLEMS

The following discussion documents the mechanical and electrical problems experienced with the AAFE unit during 3 months of operation. Considering the number of component units in the system and the fact that JPL was unable to extensively test the unit, the number of problems is not excessive. The problems encountered are described in the following paragraphs.

A small spring in the Olympus shutter mechanism broke and had to be mechanically reshaped when a single spring could not be obtained from the manufacturer. An intermittent electrical problem with the cell heater circuit was solved by replacement of a variable transformer. A problem of interaction between the sting heater current set point and the sting heater temperature measuring thermocouple has not yet been solved.

The system of magnetic reed relays for triggering the camera film advance and the Olympus shutter developed an insensitivity for one of the absorption filter positions on the processor wheel. This resulted in a double exposure because the film did not advance between processor wheel positions 4 and 5. This problem has not been solved.

Rigidity of the optical system is extremely important for schlieren photography. The technique used in the AAFE unit is clearly insufficient. This technique was to hard mount all components to mounting struts in a commercial relay rack. The rigidity problem is evident when movement of any component, such as a quarter panel door, creates sufficient warpage to move the focal point completely off the schlieren knife edge. A major design effort will be necessary to isolate and stiffen the FES to eliminate this problem. The magnitude of this problem is evident if one considers that there is a 2 m lever arm containing four turning mirrors. Since the focal spot position is critical to 20 $\mu$m or better, all components directing the light beam must be rigidly coupled.

Another feature of the rigidity problem was evident in processor wheel operation. A Geneva drive mechanism was used to turn the processor wheel. This allows the motor to turn continuously, but the processor wheel is driven

only periodically. Observation through the viewfinder revealed that the processor does not come to a smooth stop but tends to oscillate for a short time. The time delay before opening the camera shutter was insufficient to allow this oscillation to damp out. This is a problem only in the interference and schlieren mode where a component is susceptible to angular position. The easy solution of slowing down the complete process may or may not be acceptable. This will depend upon the time resolution required by the principal investigators.

Utilization of one large connector for all electrical leads (except thermocouples) made it very difficult to troubleshoot the electrical system when problems developed. Suggestions for FES development are to use several individual connectors during the development program to allow easy isolation, test, and modifications of components, and then for flight use a single connector which is automatically mated when the test cell is inserted in the test position.

# IV. OPTICAL CHARACTERISTICS

The following discussion summarizes the analysis of the optical system of the AAFE unit. A convenient format was to evaluate those characteristics specified in the Request for Proposal (RFP) which was released for development of the FES. It should be remembered, however, that the AAFE unit was not developed under the FES specifications. In fact, many things learned too late to incorporate into the AAFE unit were written into the FES RFP as performance specifications. Pertinent specifications analyzed were as follows: focus control, optical resolution at the test cell, uniformity of illumination across the test cell, light intensity and film exposure time, optical transmission of fluid and filters supplied by JPL, schlieren and interferometric sensitivity, and image distortion.

## A. Focus Control

Because of a delay in shipment of a boresight focusing mechanism for the Photosonics 16 mm camera from the manufacturer, the approach used to determine the optimum lens position for focusing on the center of the test cell was typical trial and error. Test film strips of a TV resolution chart were taken with the lens set to various distance settings. When the approximate setting was found, the TV resolution chart was replaced with a high-resolution test chart and additional film strips taken to zero in on best focus. The final result indicated that optimum focus on the test cell occurs with the lens set to 4.9 m.

This result is consistent with measured dimensions as related to the focal distance of the collimating mirror. Since the object is closer to the collimating mirror than the focal distance, the image is magnified, virtual, and upright as calculated from classical lens equations.

Before these tests were made, there was a certain amount of confusion related to focus. The lens supplied with the camera by JPL has been modified to focus "beyond infinity," i.e., to focus a converging beam. This would only be necessary if the test cell is positioned beyond the focal distance of the mirror. It now appears this modification was unnecessary. The modification does create a difference between focus distance and lens reading near infinity. This difference becomes negligible at a focus distance of 5 m.

## B. Optical Resolution

As mentioned in the previous section, a high-resolution test chart was used during the focus tests. With the resolution chart placed at the center of the test volume, it was possible to resolve lines 150 $\mu$m apart. Leaving the lens setting the same but moving the test chart forward and back 5 cm along the line-of-sight, it was found that the resolution dropped to 200 $\mu$m.

## C. Uniformity of Illumination

Uniformity of illumination of the test cell volume will be important to experiments to make quantitative measurements of fluid phenomena. Since the MSFC Image Data Processing System (IDAPS) may be used for automated data reduction, it was decided to use IDAPS to provide an indication of uniformity of illumination. IDAPS essentially digitizes a raster scan of the film with a microdensitometer. Automated statistical analysis can then be done on the digital data.

Several frames of film were analyzed on IDAPS. These frames were taken with the test cell removed. Histograms of grey scale values over selected areas of the film were used to determine the variation in film density from point to point. The grey scale values are a logarithmic representation of the film density and, therefore, a linear representation of original illumination level. The selected areas were at the center and edges of the film frame and were approximately 1.5 mm square. Statistical analysis of the data for the four frames is given in Table 1. The grey scale mean value for unexposed section of the film was 175. Note that the standard deviation is essentially an indication of film noise.

**TABLE 1. MAXIMUM AND MINIMUM GREY SCALE VALUES SELECTED FROM DIFFERENT AREAS ON EACH OF FOUR FILM FRAMES**

| Mean Grey Scale and Standard Deviation | | | |
|---|---|---|---|
| **Frame** | **Minimum Value** | **Maximum Value** | **Nonuniformity (%)** |
| A | 136 ± 2 | 143 ± 3 | 4.9 |
| B | 130 ± 2 | 141 ± 2 | 7.8 |
| C | 136 ± 3 | 147 ± 2 | 7.5 |
| D | 141 ± 3 | 147 ± 3 | 4.1 |

These results show that the AAFE unit had a nonuniformity of illumination larger than the 4 percent specified in the RFP for the FES. It should not be too difficult to meet the RFP specification. However, a difficulty will arise in interpreting film illumination on a microscale where the film noise may be of the same magnitude as image contrast.

## D. Light Intensity

The light intensity at the film plane was not measured absolutely. All measurements were made relative to an optimum exposure of the film supplied with the AAFE unit. Again, by trial and error, a setting was determined for the automatic Olympus shutter to correctly expose the film. The light source was a Hanovia 150 W compact xenon arc lamp.

The exposure time was then measured with various optical elements in the light path both with and without the filled test cell in place. The test cell was filled with a mixture of melted thymol and thymol blue. The exposure times are given in Table 2. The thymol blue is essentially opaque at 4200 Å and is highly transparent above 6000 Å (Section IV.E).

Although the exposure time is sufficiently short for most optical processes, it does not meet the RFP specifications for illumination when using monochromatic filters. The RFP for the FES specifies that there shall be sufficient light intensity to expose the film in 1 s when a 100 Å bandpass filter is used with an 80 percent absorbing medium. The data show the system is

**TABLE 2. MEASURED EXPOSURE TIMES WITH DIFFERENT OPTICAL ELEMENTS AND FILTERS IN THE AAFE APPARATUS**

| Optical Element | | | Exposure Time (s) | |
|---|---|---|---|---|
| | | | Without Test Cell | With Test Cell |
| None (Shadowgraph) | | | 0.01 | 0.06 |
| Schlieren | | | 0.03 | 0.16 |
| Interferometer (No Filter) | | | 0.10 | 0.36 |
| Filters: | Peak (Å) | Bandpass (Å) | | |
| | 6000 | 1500 | 0.04 | 0.15 |
| | 6500 | 1000 | 0.06 | 0.12 |
| | 6200 | 300 | 0.40 | 1.12 |
| | 4200 | 120 | 0.90 | >60.00 |

marginally acceptable for 100 percent transmittance. Therefore, an optical system with approximately five times the illumination should meet the FES specifications. Again, this was not a requirement for the AAFE unit, and no effort was expended by JPL to improving the illumination.

## E. Optical Transmission

One proposed use for the FES will be to study the rejection of one component of a liquid from a solidifying interface. The method of analysis would be to utilize monochromatic filters matched to the absorption edges of the liquid components. For example, as the component is rejected from the interface, its concentration will increase as will the optical absorption. The photograph through the appropriate filter would then show the concentration fields.

The AAFE unit was supplied with a fluid mixture (thymol with an unknown amount of thymol blue dye) and three broad-band optical filters. Figure 5 shows the optical absorption spectrum for the thymol, thymol blue mixture, and for the three filters. It would appear that the green filter would enhance transmission differences between the thymol and the thymol blue. No concentration gradient was visible to the eye in any photograph using any of the filters. It is not clear at this time whether the experiments were not quiescent enough or whether there is insufficient segregation between thymol and thymol blue to show up on film.

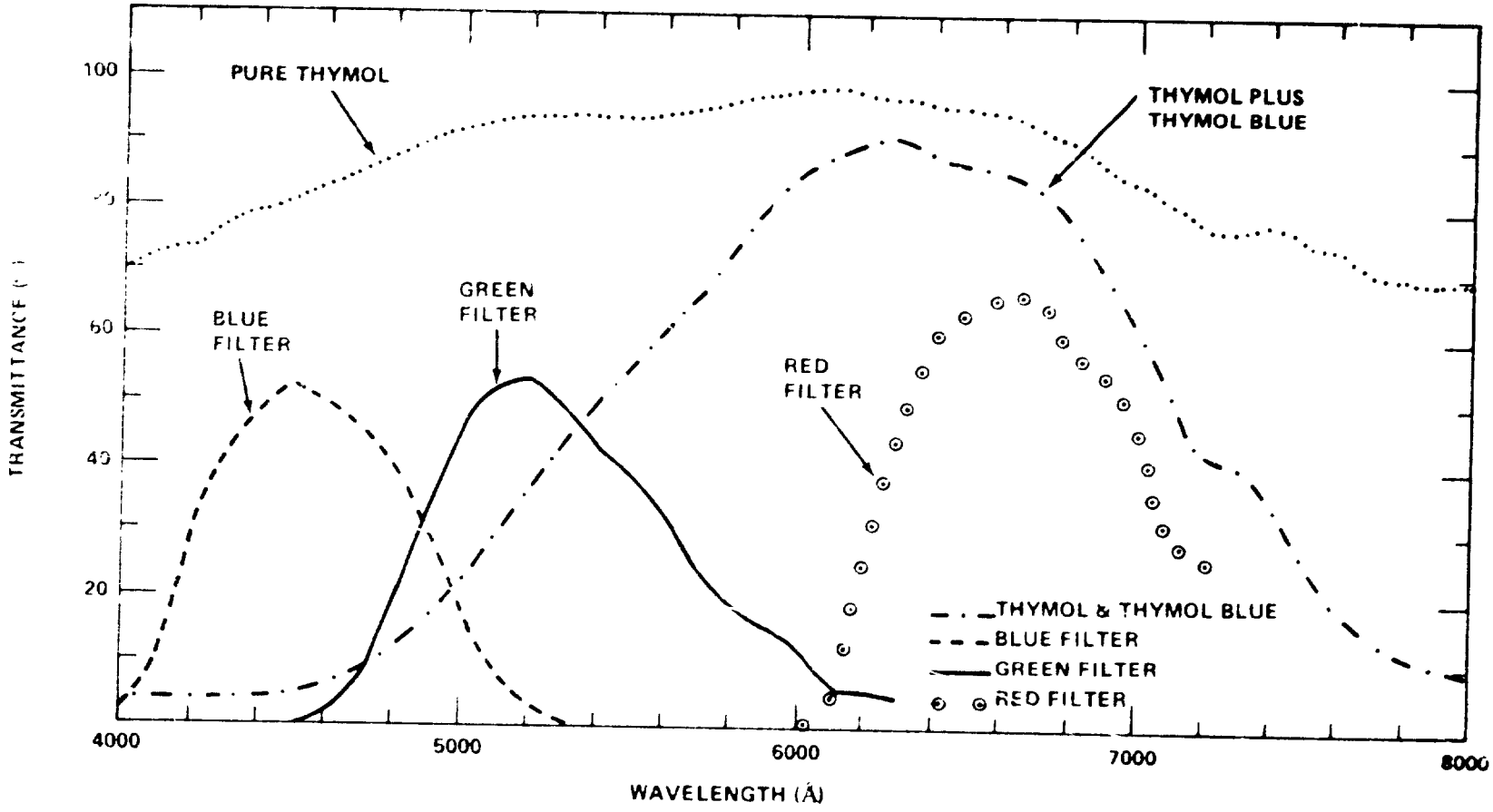


Figure 5. Optical transmittance spectra for fluids and filters supplied with the AAFE unit.

## F. Schlieren and Interferometric Sensitivity

The schlieren and interferometric characteristics were the most difficult to evaluate. The difficulties involved the inability of the crystal seed sting to work reproducibly and the inability to generate controlled temperature ramps. These difficulties made it impossible to generate quantifiable thermal or concentration gradients.

Crystals of thymol were grown by introducing a small seed into an undercooled melt. The seed crystal did grow but usually was multifaceted. Figure 6 is a photograph of one crystal taken with the schlieren knife edge in place. A plume effect is very visible. The surface of the crystal is at the melting point while the bulk fluid is at a slightly lower temperature. The warmer fluid, therefore, rises and creates a convective flow around the crystal.

Figure 7 is a photograph of another crystal using the Wollaston prism interferometer. The interferometer was adjusted to have approximately six vertically aligned fringes equally spaced across the field-of-view. Strong index of refraction gradients are visible around the growing crystal. Fringe curvature and nonuniform spacing at the cell walls indicate that the test cell was definitely not isothermal.



Figure 6. Schlieren photograph of growing crystal.

Figure 7. Interference photograph using Wollaston prism.

## V. THERMAL CHARACTERISTICS

The objective of the thermal tests was to evaluate the following characteristics of the test cells: the thermal response of the test cell and fluid, the ability to attain an isothermal condition, and the temperature stability at equilibrium.

The approach taken in the design of the test cell was to use a massive aluminum block in which the large thermal conductance would dissipate any nonuniformities in the heating. This advantage is opposed by the disadvantage of slow response due to the large heat capacity of the aluminum block.

The test cell surface temperatures were measured with the thermocouples which came attached to the test cell. The temperature readings were

taken from the digital display supplied with the apparatus. The digital display had a resolution of 1°F. This resolution is insufficient to evaluate a crystal growth system; therefore, additional instrumentation was utilized for critical measurements. The fluid temperatures were measured with a quartz crystal thermometer and a miniature thermistor (2 mm diameter glass bead). The quartz crystal thermometer has a long-term (12 month) absolute accuracy better than 0.01°C. Therefore, the thermistor was calibrated against the quartz thermometer in a variable temperature water bath. Both units have a resolution down to 0.001°C. However, only the quartz thermometer had short-term (less than 10 s) stability in the test cell at this accuracy. Since the miniature thermistor had short-term fluctuations up to 0.01°C, it must be assumed that the relatively massive (1.5 cm long by 1.0 cm diameter) quartz thermometer was averaging the short-term convective turbulence effects.

## A. Thermal Response

The question of thermal response can be divided into two aspects: (1) passive cool-down and (2) powered heat-up. The cool-down obviously depends upon the inherent heat loss mechanism, while the heat-up depends upon the heater power used and, to an extent, the heat transfer rates to the solution being heated.

The heat-up characteristics will be discussed first. Figure 8 is a photograph of the test cell with its sliding rails extended. Shown are the cell body, window flange, control thermistor, measuring thermocouples, strip heaters, and fluid stirrer attachment. The strip heaters were wired in series parallel in an effort to uniformly heat the external surfaces. The window flange also has a circumferential heating element. The temperature control system is a Tronac model PTC-36. This controller is a time-proportioning type with a thermistor sensor which has a quoted control accuracy of ±0.001°C/week. This controller applies full 110 Vac to the heating elements, with a variable duty cycle depending upon the temperature and the rate of change in the temperature.

It should be mentioned that the cell thermal measurements during these evaluations were made with no insulation blanket around the test cell. This blanket was not delivered with the test cell because of a design problem which arose in the last days of the JPL contract.

Figure 9 is a typical time-versus-temperature plot for the initial heat-up period. Shown are the curves for temperatures on a window flange, on an external cell wall surface, and at the center of the sample material volume (labeled internal). The cell wall temperature increases smoothly with no

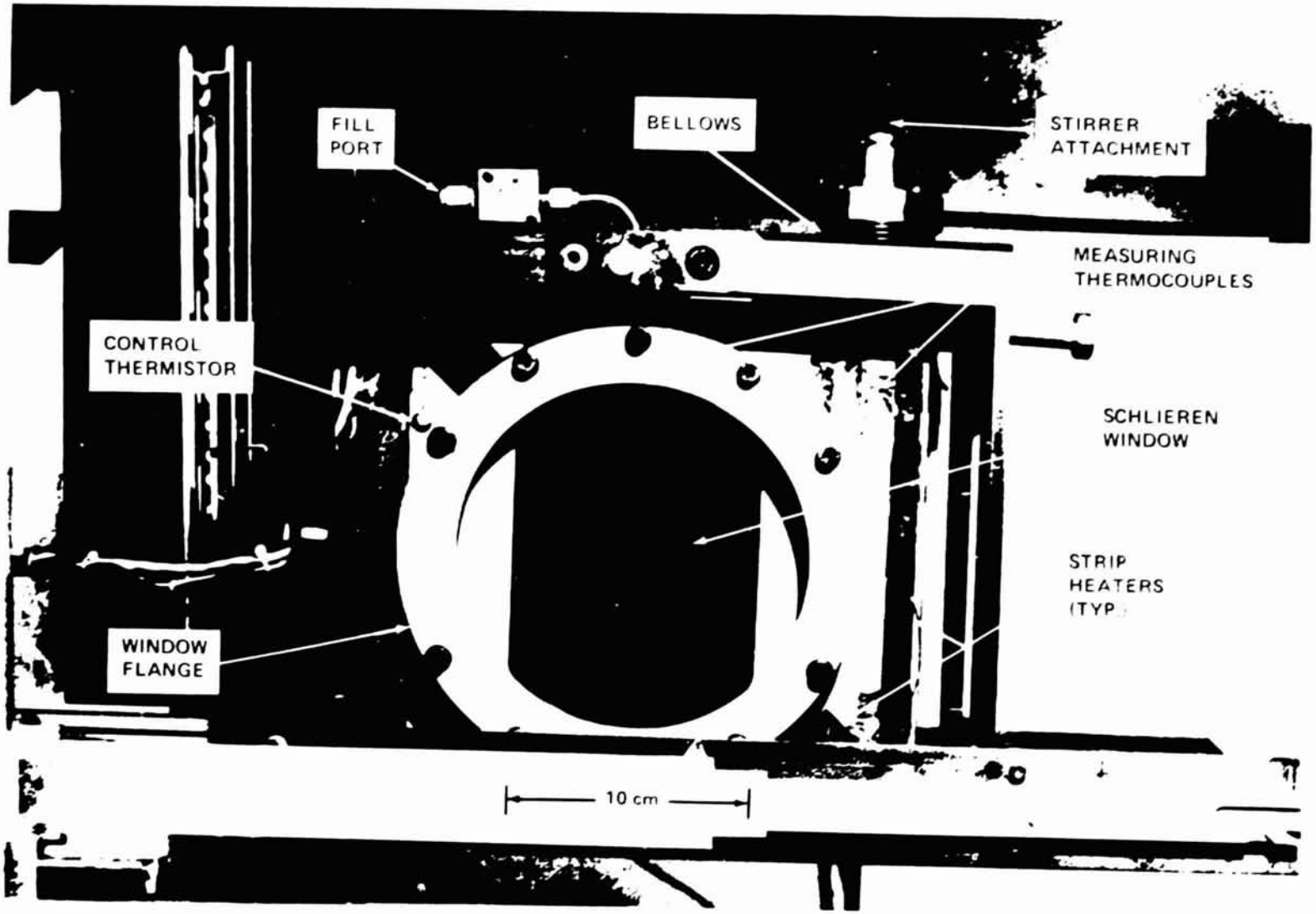


Figure 8. Photograph of test cell.

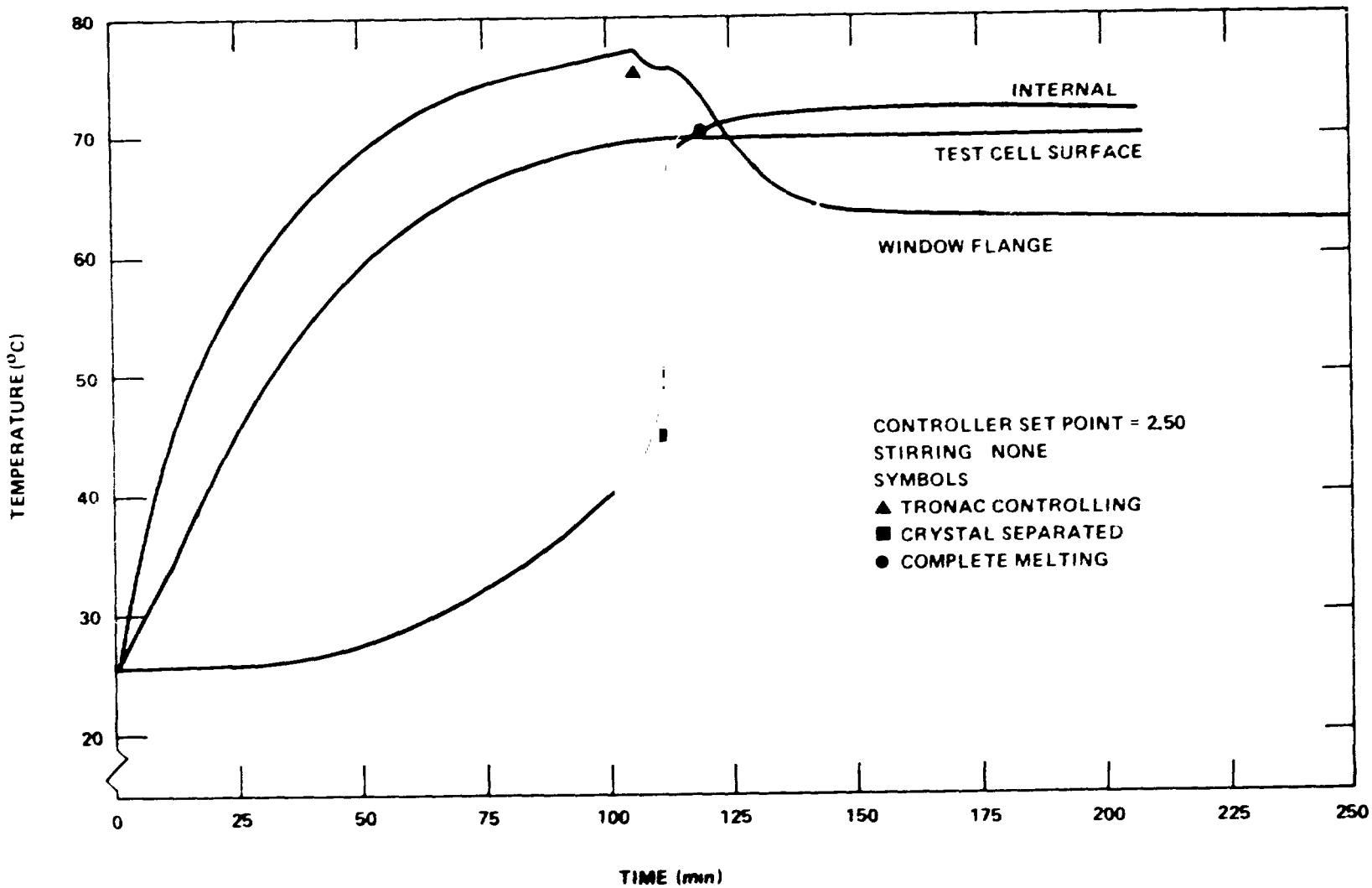


Figure 9. Typical test cell temperature during melting.

appreciable overshoot. The internal temperature lags the wall temperature due to the low conductivity of the thymol solid and to the energy absorption in the melting process. The time marking points indicate several features. The point designated by the triangle (▲), "TRONAC CONTROLLING," indicates when the wall temperature has reached the proportional band of the temperature controller. At this time, the controller begins to cut back on the time-averaged power applied to the heaters. The point designated by the square (■), labeled "CRYSTAL SEPARATED," indicates when the thymol material has melted sufficiently that it no longer encloses the temperature sensor. This obviously exposes the sensor to the fluid which is at a temperature above the melting point. The point designated by the circle (●), labeled "COMPLETE MELTING," indicates when all solid material has melted. Since the thymol mixture melts at 48°C, it is obvious that the bulk of the liquid can be at higher temperatures while solid material still exists.

The main conclusion which can be drawn from the window flange temperature curve is that a separate temperature controller is needed. During heat-up the flange is considerably hotter than the cell proper because the flange is not in good thermal contact with the melting material. Once the sample is melted and the average power applied is cut back, the flange becomes colder than the cell because of its large convective heat loss to the surrounding air. Therefore, protuberances with different heat loss mechanisms must be individually controlled because the technique of using a fixed percentage of the total heat would be correct for only one temperature set point. It should also be noted that an extremely long time (300 min) is required for the window flange to reach a stable temperature as compared to the cell (125 min).

Figure 10 is a temperature-versus-time plot showing the influence of temperature set points on melting time. The controller set point was varied for each of three runs while all other parameters were held constant. The stirrer for mixing the fluid after it starts melting was set at 40 percent of its range. As was expected, the higher the cell wall temperature, the faster the sample melts. Obviously, a larger gradient between the cell surface and the crystal will provide a higher energy flow rate for the melting process.

This has several implications for developing a protocol for melting samples in a Spacelab experiment. Saving time from such unproductive activities as melting samples will be very important for maximizing the actual experiment time. This is especially true for solution crystal growth techniques which typically take days to weeks on Earth. Obviously, setting a very high cell wall temperature will speed up melting. However, a limit will be reached when liquid in contact with the cell wall will attain temperatures which are unacceptable. The technique to maximize the benefit while minimizing the problems is to

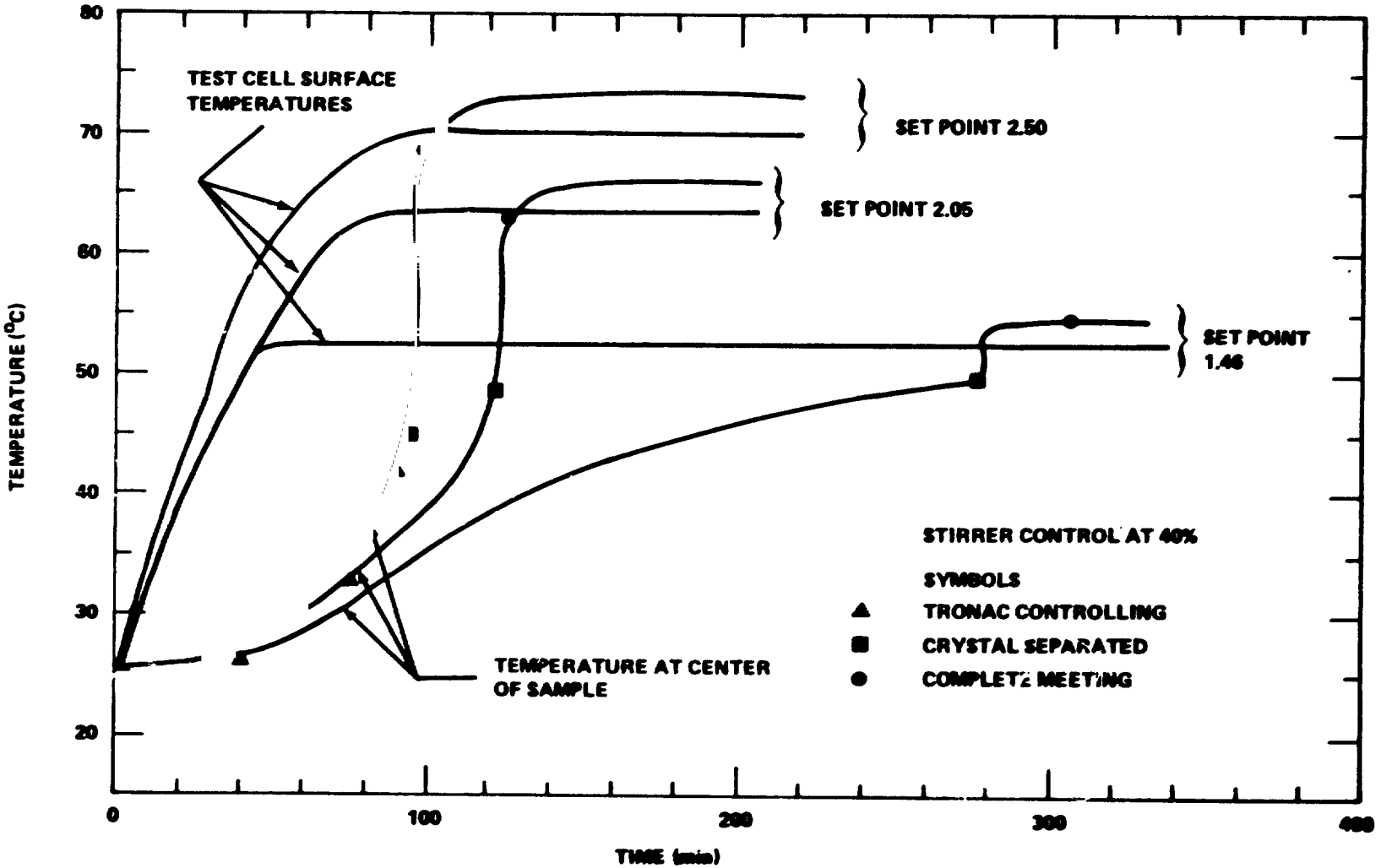


Figure 10. Fluid temperatures during melting as function of temperature controller set point.

put the controlling temperature sensor in the sample near the hottest cell wall surface. This technique of driving the liquid temperature well above the melting temperature is compatible with many potential crystal growth experiments. Usually, it is desirable to soak the solution at a temperature above the melting point to insure uniformity of the solution.

Another method for speeding up the initial melting process is to use a liquid stirrer. Figure 11 shows the effectiveness of the stirrer built into the test cell. The lower set of curves shows time versus temperature for three stirrer speed settings, all at a temperature control set point 3°C above the melting point. At this set point, the time for complete melting was reduced by 50 percent by changing to the 63 percent stirrer speed setting. The upper set of curves shows that the same stirrer range is much less effective at a higher temperature set point. Although not very effective for reducing time to melt at high set points, a high stirrer speed will always tend to reduce thermal gradients in the fluid.

The thermal response of the test cell was also measured for small step changes in the set point once the sample was melted and at equilibrium. Figure 12 is a typical time-versus-temperature plot for a step change (both cooling and heating). The figure shows the cell wall temperature and the fluid temperature at the center of the cell. It can be seen that upon heat-up the test cell reaches equilibrium in approximately 50 percent of the time it takes for the fluid to reach equilibrium. Equilibrium has been arbitrarily defined as reaching 0.1°C of the final temperature. On cool-down, the fluid tracks the cell wall temperature much closer. The controller has a slight overshoot in both the heating and cooling mode. This overshoot on the cell outside surface is damped out before it reaches the center of the fluid.

The following was concluded from a series of step changes in temperature:

1) The stirrer speed does not appear to appreciably affect the time to reach equilibrium on either heat-up or cool-down.

2) At higher temperatures, the maximum heat-up rate is reduced while the maximum cool-down rate is increased, indicating the heat losses to the ambient are an appreciable fraction of the maximum power available from the heaters, as is expected with no insulation around cell.

3) For a cell of this mass, at least 1 h should be scheduled to reestablish equilibrium after a step function change in temperature.

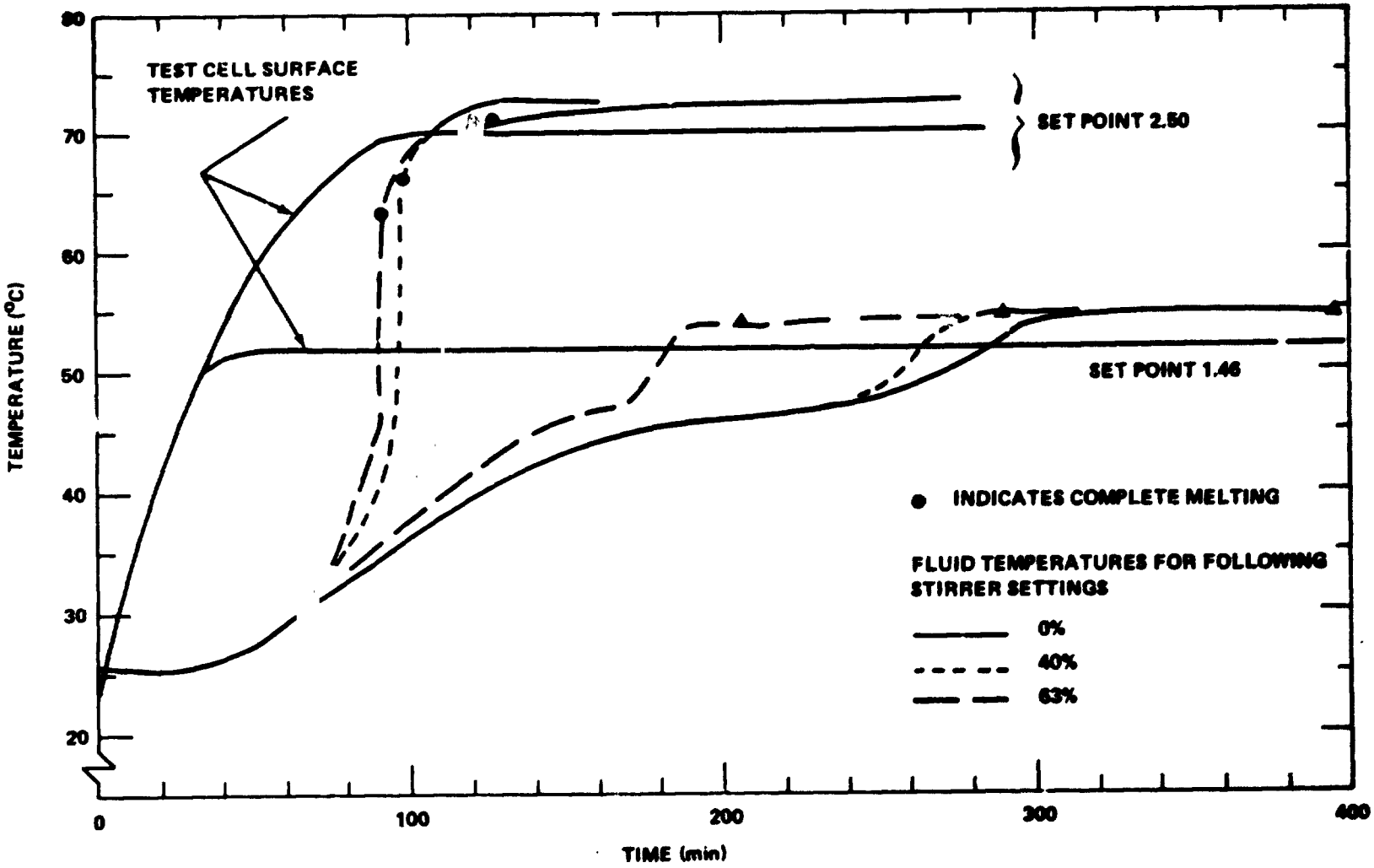


Figure 11. Fluid temperatures during melting as function of stirrer rate for low and high temperature set point.

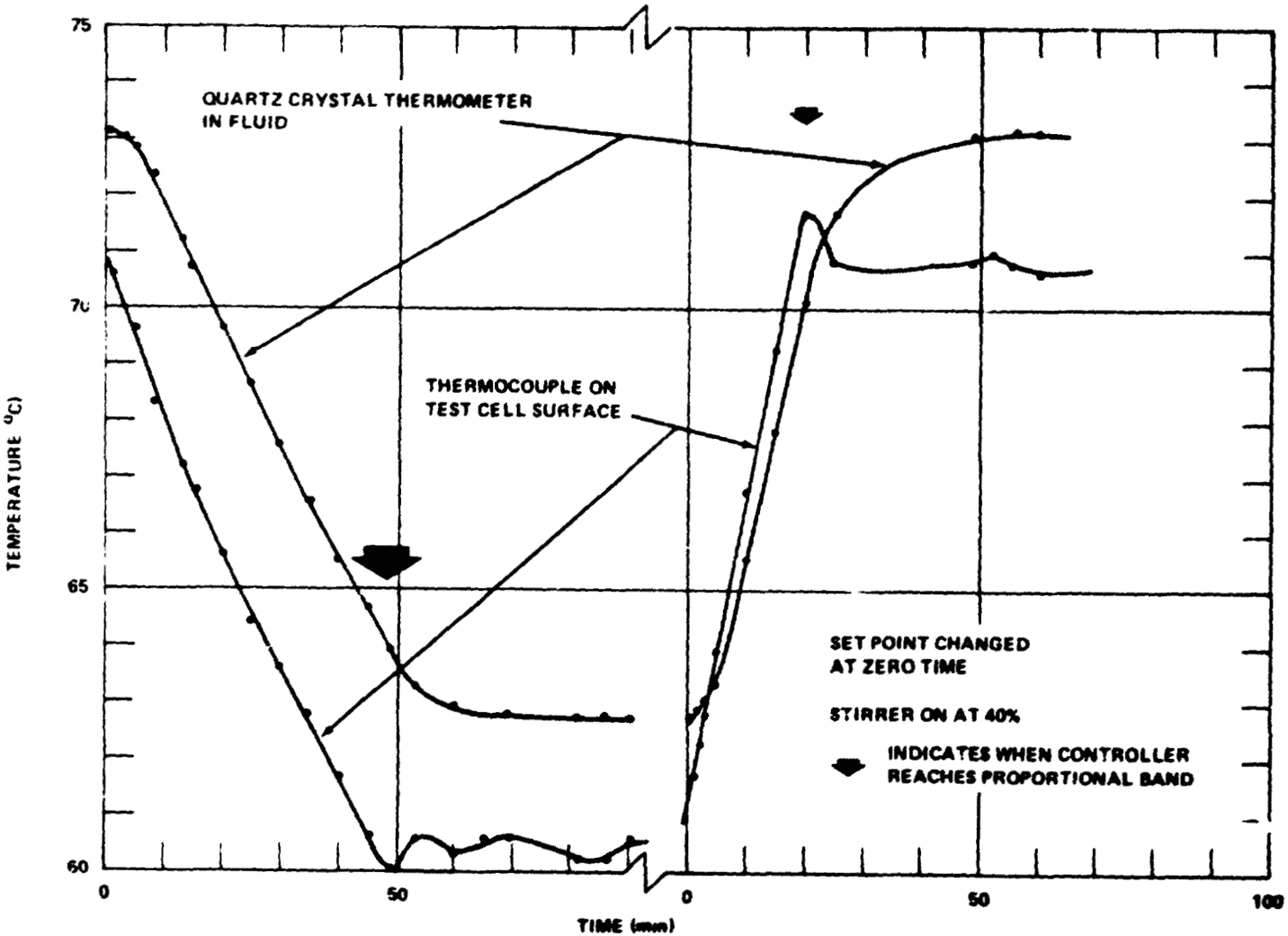


Figure 12. Temperature response to controller set point change.

## B. Temperature Uniformity

Profiles were made of the temperature distribution within the test cell. The miniature thermistor was used as the moveable temperature probe. All measurements were made several hours after a given set point temperature was reached and the stirrer stopped.

Figures 13 and 14 show typical profiles taken horizontally and vertically through the center of the test cell, respectively. From Figure 13 it can be seen that the fluid temperature from side to side of the test cell varies no more than 0.1°C, except at the extreme edge. The decrease at the wall exposed directly to air is reproducible and indicates a sinking convective flow.

Figure 14 shows the relatively large thermal stratification which exists in the vertical direction. The 2.3°C differential shown in this test was typical of several different tests. The very small reverse gradient at the liquid-air interface is also reproducible but is believed to be due to cooling of the thermistor through the electrical leads.

An obvious and very necessary follow-on to this test will be to design an insulation jacket for the test cell and repeat these tests.

Temperature profiles were also measured in the vicinity of the window flange at the bottom of the cell. As expected, the fluid was also approximately 0.5°C cooler than the bulk fluid because the window flange is cooler than the cell walls at equilibrium. This effect was limited to an area within 1 cm of the flange, however. The fluid next to the window was an additional 0.3°C cooler than the flange.

Whether these nonuniformities can be eliminated by insulation alone or whether active control of the window and window flange is necessary is also a subject for further tests.

## C. Temperature Stability

The characteristic of temperature stability is very critical for potential experiments such as crystal growth. Figure 15 is a graph of a time-versus-temperature measurement taken at the center of the test cell. Zero time is when the stirrer was stopped. Prior to this time, the sample has been melted and equilibrium established. This test was chosen for display because it was the most uniform and had the longest episode of isothermal condition. It can be

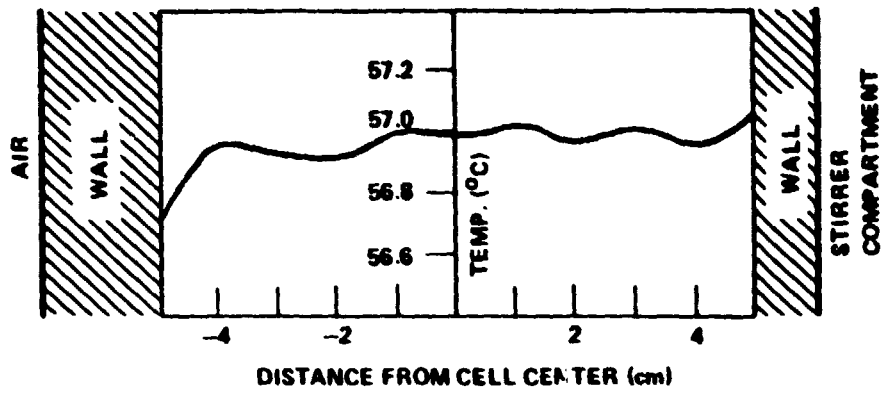


Figure 13. Horizontal temperature profile at midline of test cell.

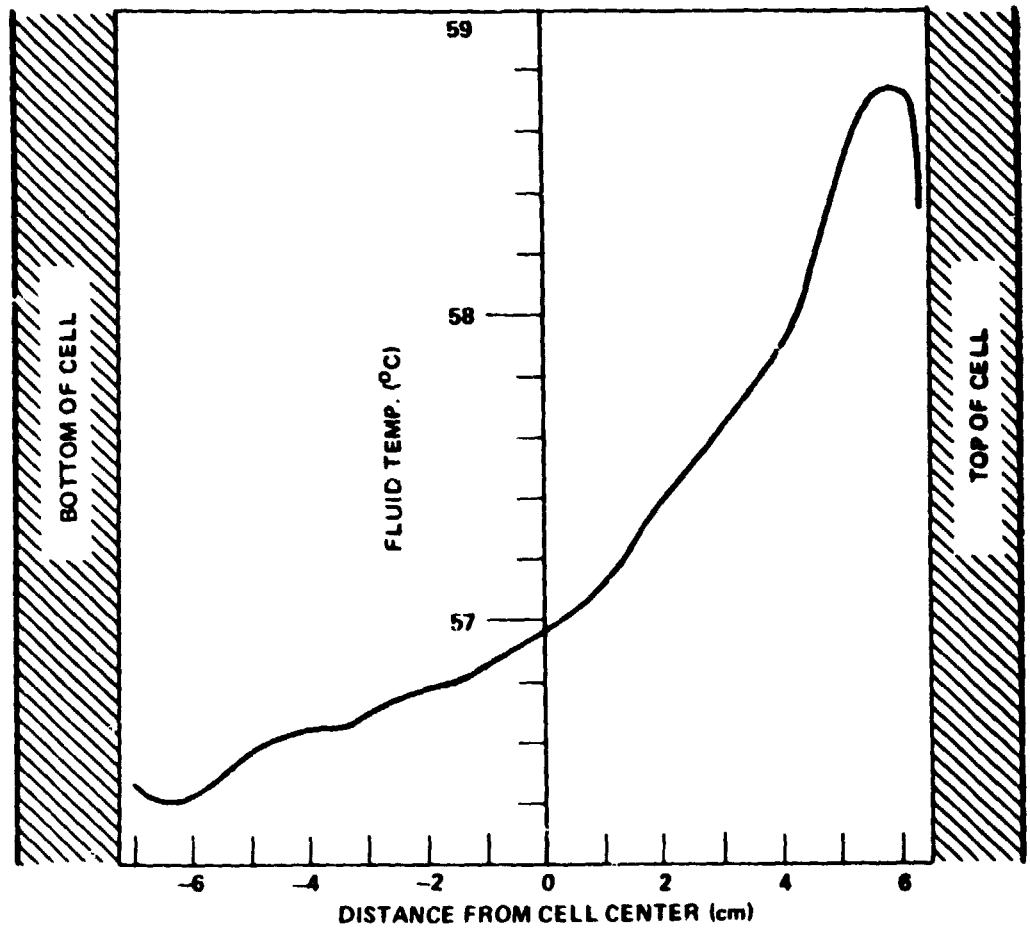


Figure 14. Vertical temperature profile at midline of test cell.

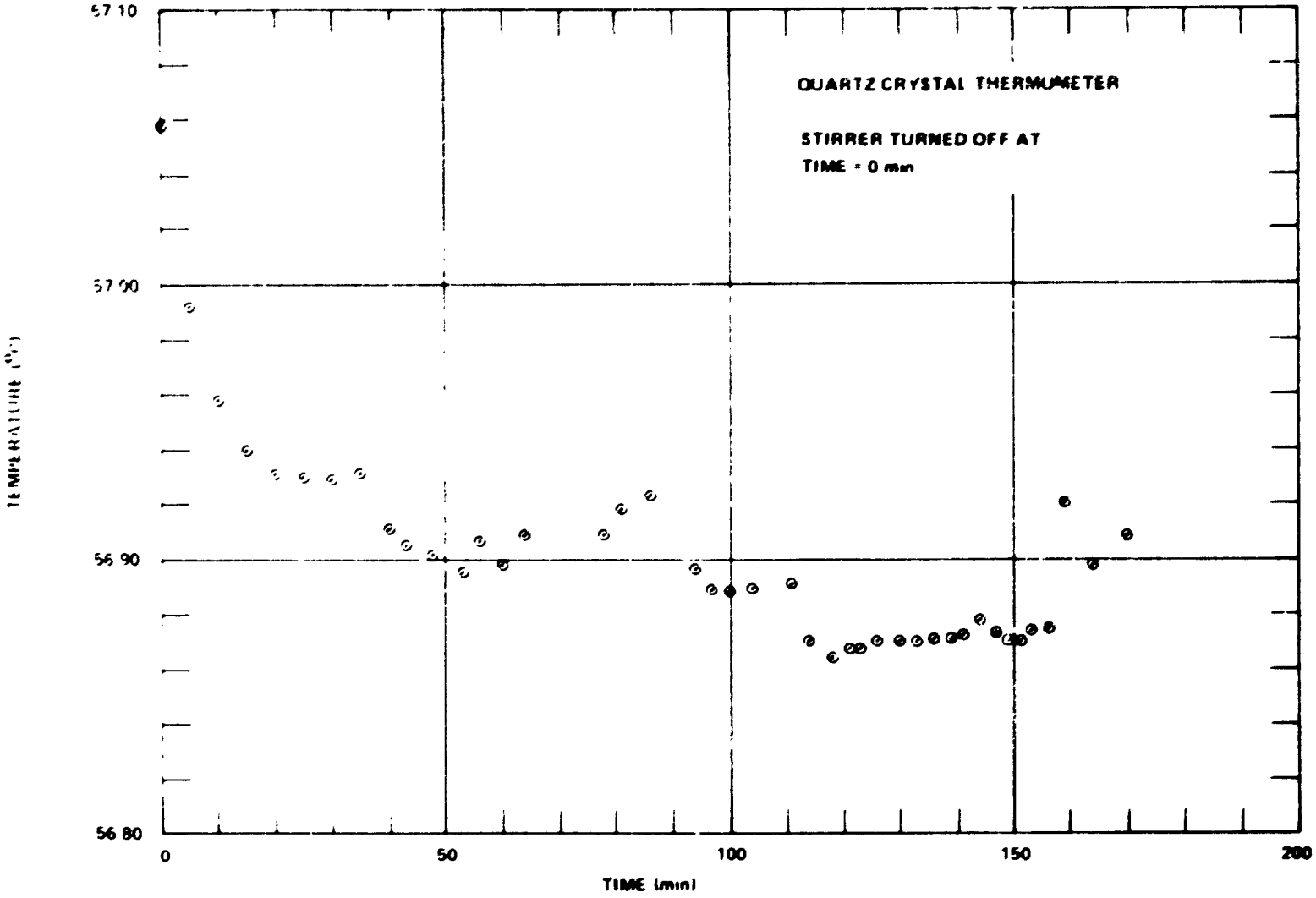


Figure 15. Time versus temperature at center of fluid in test cell.

seen that it takes approximately 30 min for the fluid to stabilize after turning off the stirrer. After this time, there appears to be random fluctuations in the mean temperature. The data shown were taken with the quartz crystal thermometer and show fluctuations of 0.03°C about an overall average. Surprisingly, data taken with the miniature thermistor probes showed fluctuations of ±0.04°C. The implication is that the temperature fluctuations are a large-scale fluid readjustment rather than small-scale wandering convective plumes.

Considering the magnitude of the thermal gradients in the test cell which were shown to exist in the previous section, these temperature fluctuations are definitely not excessive. It is anticipated that by insulating the test cell the convective instabilities can easily be brought below 0.01°C. The value of 0.01°C was specified as the minimum control and resolution for the FES.

# VI. SUMMARY OF RECOMMENDATIONS FOR SECOND GENERATION APPARATUS

The following is a summary of recommendations more fully described in previous sections:

a) Experiment operators (Spacelab Payload Specialists) must be trained in optical alignment procedures.

b) All mechanical adjustments must be identified and positioned for easy operator access.

c) The mechanism for selecting processor wheel positions should be versatile. For example, the option of taking photographs through only one element should be available without the need to cycle through all six elements. Also, the framing rate should be adjustable.

d) A mechanism must be developed to allow the operator to accurately focus the camera lens on the film plane.

e) The camera position should be such that it is convenient to both load film and focus without jarring the apparatus.

f) All temperature measurement and control apparatus should be direct reading in degrees Celsius rather than in arbitrary units.

g) Data display on film is a necessity. A mechanism for controlling data display intensity to match image intensity is required.

h) The following experimental techniques must be developed for crystal growing experiments: crystal nucleating device, seed insertion and crystal removal mechanisms, bubble removal and control mechanisms, adjustable temperature probes, controllable temperature gradient plates, and controllable temperature-versus-time profiles.

i) The mounting structure for the optical components must be very rigid.

j) During development of the FES, it is recommended that individual electrical connectors for all components be utilized to facilitate isolation, test, and modifications. The flight unit should, however, use a single, automatically mated connector.

k) The processor wheel should have minimum vibration, and the camera trigger should be delayed until all residual vibration is gone.

l) Depending upon the test cell thermal characteristics, a protocol must be developed for preheating and melting the sample while using a minimum of the FES time line; i.e., the time for productive crystal growth must be maximized.

## VII. SUMMARY OF TEST RESULTS

The specific test results have been discussed in earlier sections. This section summarizes the performance of the AAFE apparatus as compared to the performance specification given in the RFP for the FES. It should be reemphasized that the AAFE development helped define the performance specifications for the FES and that no time or resources were ever devoted to optimizing the performance of the AAFE apparatus to meet the FES criteria.

The thermoelectric plates for creating thermal gradients in the test cell fluid appear to heat and cool the fluid quite well. However, the plates are vertical with no mechanism for turning the cell on its side to generate a thermally stable gradient (hot side up). The FES must incorporate a mechanism for varying the thermal plate positions.

The AAFE apparatus can resolve lines 150 $\mu$m apart at the test cell. Since there is approximately a 10 to 1 reduction to the 16 mm film, the resolution

is approximately 15 μm on the film. This is within a factor of 2 of the ultimate resolution of most commercial film. For the FES, the film should be the limiting factor on resolution.

Four frames of film were analyzed to determine the uniformity of illumination with no test cell in place. The maximum nonuniformity from point to point on each frame ranged from 4.1 to 7.8 percent. This is near the limit of 4 percent specified for the FES.

The 150 W compact xenon arc lamp was barely able to correctly expose the film in 1 s through a 100 Å bandpass filter with no test cell. The FES specification is the same but with an 80 percent absorbing medium. Therefore, the AAFE apparatus would need approximately five times more intensity. This does not appear to be a difficult specification to reach since only a small concentration lens was used in the AAFE system.

The ability to detect concentration gradients of colored impurities could not be measured. It is not known whether the convective mixing washed out the segregated diffusion layer or whether the segregation was too small to show up on film.

The schlieren and interferometric sensitivies could not be quantified, although they were observed. The test cell did not lend itself to making and quantifying a stable thermal gradient which could be related to a certain schlieren and interferometric effect. This again points up the need for a test cell which can be used to quantify thermal and concentration gradients.

The temperature control system for the test cell must incorporate separate controllers for every surface which has different heat loss characteristics. A surface such as the AAFE window flange has widely varying temperatures from the basic test cell if only a fixed percentage of power is provided to the flange.

The time to reach equilibrium from room temperature varied from 2 to 6 h, depending upon the temperature set point and whether a fluid stirrer was used. These results were obtained with a 100 W heat input until the test cell exterior surface reached the set point.

The time to reach equilibrium after a 5 or 10°C temperature step is approximately 1 h. The fluid stirrer did not appreciably change the time to reach equilibrium on either heat-up or cool-down.

After the test cell temperatures have stabilized, a 2.3°C thermal differential exists from the bottom to the top. The horizontal differential is approximately 0.1°C. The large vertical gradient is the obvious result of not having any insulation on the test cell surface. The FES specification is for isothermal conditions to 0.01°C. This will necessitate both insulation and individual heater controls on different surfaces.

Even with the large vertical thermal gradient, the temperature stability at a given point was within ±0.04°C. It appears that when the thermal gradient is reduced, it may be relatively easy to control the fluid to 0.01°C as specified for the FES.

# APPROVAL

## EVALUATION OF AAFE APPARATUS TO MEASURE RESIDUAL AND TRANSIENT CONVECTION IN ZERO-GRAVITY

By R. C. Ruff, B. R. Facemire, and W. K. Witherow

The information in this report has been reviewed for technical content. Review of any information concerning Department of Defense or nuclear energy activities or programs has been made by the MSFC Security Classification Officer. This report, in its entirety, has been determined to be unclassified.

Lewis Lacy

LEWIS L. LACY
Chief, Solid State Branch

Robert J. Naumann

ROBERT J. NAUMANN
Chief, Space Processing Division

Charles A. Lundquist

CHARLES A. LUNDQUIST
Director, Space Sciences Laboratory

☆ U.S. GOVERNMENT PRINTING OFFICE 1978 740 193/112 REGION NO. 4